water

MDPI

Article

Impact of Phytoplankton Community Structure Changes in the South Sea of Korea on Marine Ecosystems Due to Climate Change

Kyung-Woo Park [1], Mi-Hee Chung [2], Man-Ho Yoo [3], Kwang-Seok O [4], Kyoung-Yeon Kim [1], Tae-Gyu Park [1] and Seok-Hyun Youn [1,*]

[1] Oceanic Climate & Ecology Research Division, National Institute of Fisheries Science, Busan 46083, Republic of Korea; kyungwoopark@korea.kr (K.-W.P.); weedy7411@korea.kr (K.-Y.K.); taegyupark@korea.kr (T.-G.P.)
[2] Marine Micro Algae Research Institute, Busan 48081, Republic of Korea; aloisia91@gmail.com
[3] HAERANG Technology and Policy Research Institute, Suwon 16229, Republic of Korea; u10005@haeri.co.kr
[4] Haeon Plankton Ecology Research Institute, Busan 48106, Republic of Korea; ghangsok79@gmail.com
* Correspondence: younsh@korea.kr; Tel.: +82-51-720-2233

Abstract: Herein, we conducted surveys during the 2018–2022 summers to investigate the impact of climate change-related changes in the phytoplankton community structure on the marine ecosystem in the South Sea of Korea. The average surface water temperature increased by ~1.07 °C at 0.0195 °C·yr^{-1} between 1968 and 2022. During the summers, the rate was 0.0211 °C·yr^{-1}, with a total increase of ~1.16 °C, indicating a stronger increase in summer surface water temperature. Over the last 30 years, nutrient levels in the South Sea have decreased, particularly at the surface. Moreover, 29.3–90.0% of the phytoplankton community structure was dominated by nanoflagellates (≤20 μm). Based on the size of the phytoplankton chl-*a*, the average contribution rate of picophytoplankton was the highest (60.1%). Redundancy analysis revealed negative correlations between nutrients and water depth, excluding NH_4. Increased stratification due to climate change is causing reduced nutrient availability at the surface mixed layer, and the size of the phytoplankton structure is progressively reducing. These changes are expected to manifest in a complex microbial food web centered on smaller phytoplankton with low primary productivity. This can reduce the efficiency of carbon transfer to higher consumer levels, suggesting a potential decrease in marine productivity.

Keywords: South Sea of Korea; climate change; phytoplankton community; chl-*a* size fraction; picophytoplankton; reduced nutrients

Citation: Park, K.-W.; Chung, M.-H.; Yoo, M.-H.; O, K.-S.; Kim, K.-Y.; Park, T.-G.; Youn, S.-H. Impact of Phytoplankton Community Structure Changes in the South Sea of Korea on Marine Ecosystems Due to Climate Change. *Water* **2023**, *15*, 4043. https://doi.org/10.3390/w15234043

Academic Editor: Yuqiang Tao

Received: 23 October 2023
Revised: 18 November 2023
Accepted: 20 November 2023
Published: 22 November 2023

1. Introduction

According to comprehensive reports by the Intergovernmental Panel on Climate Change (IPCC), the global warming trend is accelerating. Assessment Report 5 (AR5) presents climatological data indicating that the global surface temperature has increased by 0.85 °C since the Industrial Revolution, while the most recent report, AR6, indicated a more significant increase of approximately 1.1 °C [1]. Marine heatwaves have occurred in various sea areas around the world over the past 20 years and are inevitably affecting marine ecosystems by causing die-offs of myriad marine organisms, including coral reefs, kelp, algae forests, fish, and seabirds [2,3]. The overall decrease in fishery production is also influenced by these phenomena. Although making highly reliable predictions regarding fishery production is challenging for mid-latitude oceanic regions such as South Korea, a 10–15% decline has been projected due to model uncertainties and regional variations [3]. The World Meteorological Organization (WMO) has indicated that key ocean-related indicators of climate change are rapidly increasing, suggesting that its impact on marine ecosystems will accelerate [4].

Phytoplankton are crucial primary producers in the marine food web. The community structure and primary productivity of phytoplankton are influenced by the distribution characteristics of water masses, changes in environmental factors, and top predator feeding. Phytoplankton serve as an important indicator of the impact of recent climate-induced oceanic physical and chemical changes on marine ecosystems [5,6]. Moreover, the long-term variability of phytoplankton is a highly significant indicator for studying ocean resource fluctuations and predicting the impacts of climate change on human activities. Therefore, understanding the occurrence patterns and distribution characteristics of phytoplankton is crucial to comprehending the changes in marine environments and water mass structures due to climate change, as well as for understanding the energy-transfer processes throughout the food web [7].

The South Sea of Korea is a general term for the sea located to the south of Korea. In terms of international maritime law, it is considered part of the East Sea, Yellow Sea, and East China Sea. The South Sea of Korea is influenced by various water masses (depending on the season), including Korea's unique coastal waters, the cold bottom layer of the Yellow Sea, diluted water from China's Yangtze River, and the Tsushima Warm Current originating from the Kuroshio Current. The South Sea of Korea also contributes to the regulation of seawater circulation by transporting heat, salt, and nutrients to the East Sea [8–11]. In addition, it is a critical area for the fisheries industry, featuring a vast distribution of fishing grounds; in particular, it is a migration habitat for coastal migratory fish species [11].

The concentration of surface nutrients continues to decrease due to the strengthening of the ocean surface stratification [12,13], resulting in phytoplankton miniaturization [14–16]. Recently, primary productivity in Korean waters has exhibited a rapidly decreasing trend, with phytoplankton miniaturization purported to be the primary contributing factor [17–19]. Indeed, small phytoplankton play an important role in primary productivity and the marine ecosystem food web [18,20–23]. However, past research on phytoplankton in the South Sea has primarily focused on the coastal region, with relatively limited studies reporting the phytoplankton community structure during specific periods in the nearshore areas [11,24–30]. Consequently, research on small phytoplankton in the South Sea is limited.

Accordingly, the primary objective of this study is to evaluate how climate change-related alterations in the marine environment impact the phytoplankton community structure in the South Sea of Korea. Moreover, we consider the impact of changes in the phytoplankton community structure on the marine ecosystem.

2. Materials and Methods

2.1. Cruises and Sampling

To investigate the phytoplankton distribution in the South Sea of Korea during the summer, we conducted five surveys from 2018 to 2022 using the National Institute of Fisheries Science's research vessel, Tamgu 8 (283 ton), at 12 sampling stations (Figure 1, Table 1). To quantify phytoplankton and nutrient concentrations, we first collected samples at seven depths (0, 10, 20, 30, 50, 75, and 100 m) using a Niskin sampler (8L PVC, General Oceanics, Miami, FL, USA) attached to a conductivity, temperature, and depth CTD/rosette sampler. Vertical temperature and salinity distributions were measured using a calibrated SBE 9/11 CTD sampler (Sea-Bird Electronics, Bellevue, WA, USA), and analysis was performed using the down data.

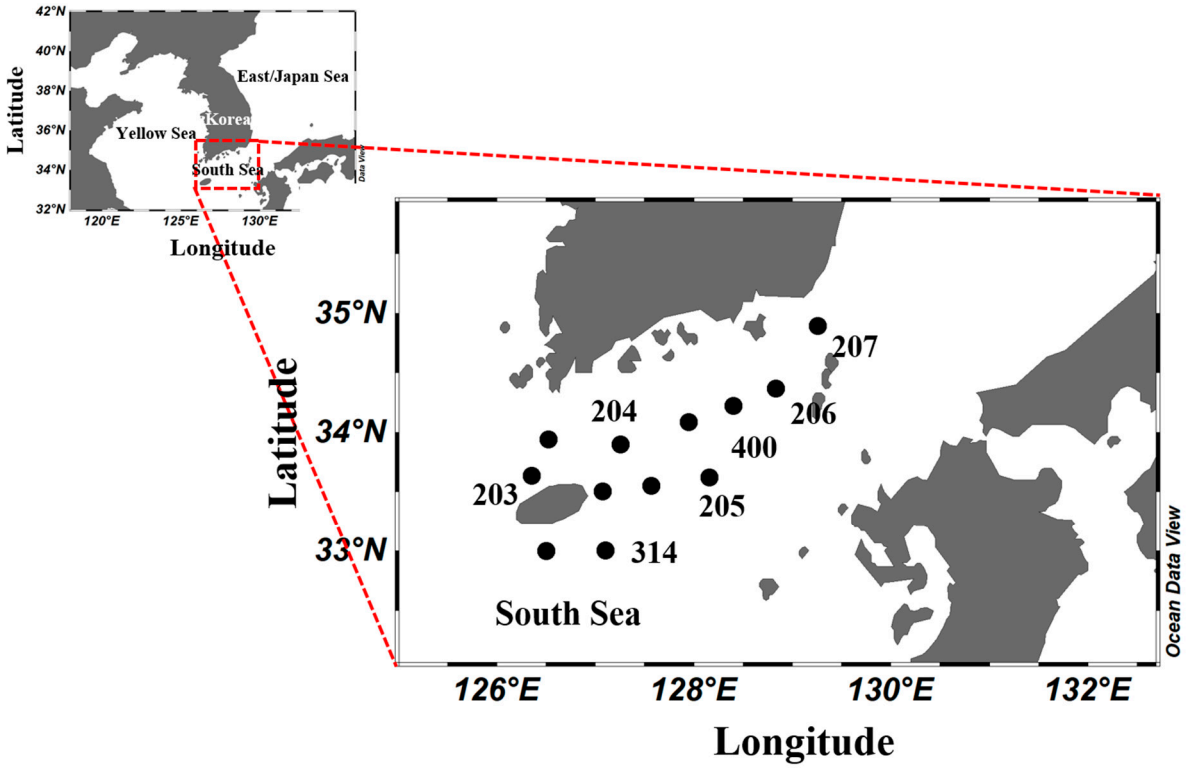

Figure 1. Sampling stations (numbered in the expanded view) in the South Sea of Korea from 2018 to 2022.

Table 1. Description of the sampling sites in the South Sea of Korea used during the cruise period (2018–2022).

Station	Latitude	Longitude	Bottom Depth (m)
203-01	33.9	126.5	55
203-03	33.6	126.3	141
204-04	33.9	127.2	81
205-03	34.1	127.9	81
205-05	33.6	128.1	120
206-03	34.4	128.8	102
207-03	34.9	129.2	130
314-03	33.0	127.2	107
314-05	33.0	126.5	108
400-14	34.2	128.4	84
400-25	33.5	127.5	102
400-27	33.5	127.1	127

2.2. Dissolved Inorganic Nutrients

For the nutrient analysis, a fixed volume of seawater (10 mL) was filtered through a membrane filter (0.45 µm disposable membrane filter unit, ADVANTEC, Tokyo, Japan) and stored in a conical tube (15 mL) rinsed with hydrochloric acid (HCl, 10%). The samples were immediately frozen and stored at −20 °C. Subsequently, the samples were thawed at room temperature (20 ± 2 °C) and analyzed for ammonia nitrogen (NH_4), nitrite nitrogen (NO_2), nitrate nitrogen (NO_3), phosphate (PO_4), and silicate (SiO_2) contents using an automated nutrient analyzer (Quaatro, Seal Analytical, Norderstedt, Germany). The sum of the NH_4, NO_2, and NO_3 concentrations was calculated as the dissolved inorganic nitrogen (DIN).

2.3. Mid- to Long-Term Data on Surface Water Temperature and Nutrients

We investigated changes in the long-term annual summer SST and nutrient trends in the South Sea of Korea. We used SST data obtained from 1968 to 2022 (SST) and 1993 to 2022 (nutrient) collected by the National Institute of Fisheries Science (NIFS) and serial oceanographic observations (NSO) from the Korea Oceanographic Data Center (KODC; https://nifs.go.kr/kodc/eng/index.kodc; accessed on 17 May 2023.).

2.4. Phytoplankton Abundances and Dominant Species

To quantify phytoplankton, samples were collected at standard depths and preserved in a 1-L square container (polyethylene bottle) using Lugol's solution (final concentration: 1%). These samples were transported to the lab and left to settle for 2 days before being concentrated to a primary volume of 200 mL. Subsequently, the samples were transferred to a settling cylinder and left to settle for another 2 days and concentrated to a final volume of 20 mL. Phytoplankton in the concentrated samples were identified and counted using an optical microscope (Nikon Eclipse, Ni-U) at magnifications ranging from 100× to 1000× using a Sedwick–Rafter chamber [31–34]. The data were converted to tcells·L^{-1} unit, and species that accounted for >5% of the total abundance were classified as dominant.

2.5. Chlorophyll-a (Chl-a) Size Fractions

The fundamental methods and calculations used to determine the chl-*a* concentration were based on the method suggested by Parson et al. [35]. In brief, to measure chl-*a* concentrations in phytoplankton by size (micro: >20 µm; nano: 20 µM ≥ chl-*a* ≥ 3 µm; pico: chl-*a* < 3 µm), 0.5 L of water was sequentially filtered through filter holders equipped with a 20-µm membrane filter (polycarbonate [PC]-track etched membrane disk, 47 mm diameter, General Vacuum System, USA), a 3-µm PC membrane filter (47 mm diameter, Whatman, Florham Park, NJ, USA), and a 0.45-µm membrane filter (47 mm diameter, ADVANTEC, Tokyo, Japan). The chl-*a* values were obtained for the micro-, nano-, and pico-sized fractions, and the total chl-*a* concentration was calculated by adding these three fractions. Each filter paper was stored at −80 °C and transported to our laboratory, where they were submerged in 90% acetone and kept in the dark for 24 h to extract the chl-*a*. Afterward, particulates and the extraction filter were removed using a syringe filter (0.45 µm, PTFE, Advantec, Florham Park, NJ, USA). The absorbance was measured using a 10-Au fluorometer (Turner Designs, San Jose, CA, USA) calibrated with a chl-*a* standard (Sigma, Darmstadt, Germany). Data obtained during 2022 were excluded due to sampling errors. We determined the size index (SI) based on the protocol proposed by Bricaud et al. [36] to explore the relationship between phytoplankton size and geographical distribution using the chl-*a* values obtained from each size fraction. Although the SI is a rough indicator of this relationship, it offers a single parameter that characterizes the size structure of the phytoplankton community [37]. The SI was calculated using the following equation:

$$SI = (1 \times [\%\ picophytoplankton] + 5 \times [\%\ nanophytoplankton] + 50 \times [\%\ microphytoplankton])/100$$

2.6. Data Analyses

We used the R statistical program (version 4.0.3) to analyze statistical correlations between environmental factors and phytoplankton groups collected in the northern waters of the East China Sea. Based on the results obtained using the decorana function of the R statistical package, which showed that the length of the DCA1 axis was <3 (1.23719), we conducted statistical analyses using redundancy analysis (RDA).

3. Results

3.1. Physical Environment

The average distribution of surface water temperature in the South Sea during August was 23.5–28.6 °C, with an overall average of 27.4 ± 1.4 °C, displaying higher temperatures at stations influenced by the Tsushima Warm Current (Figure 2a). The surface salinity

distribution ranged from 30.9 to 32.4, with an average of 31.7 ± 0.4, with lower values in the western waters and higher values in the eastern waters (Figure 2b). Vertically, the average water temperature ranged from 13.0 to 28.6 °C, with an overall average of 21.4 ± 5.0 °C. A thermocline formed at 10–30 m (Figure 3a). The average salinity ranged from 30.9 to 34.5, with an overall average of 33.0 ± 1.0 (Figure 3b). In the western waters, low salinity levels <32.0 were observed between the surface and 20 m, which appeared to be influenced by the influx of low-salinity water from the Yangtze River in the summer.

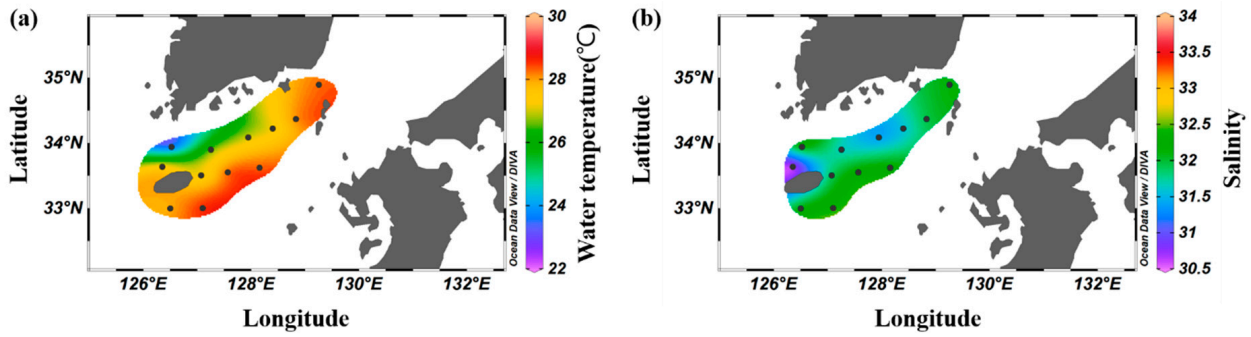

Figure 2. Spatial distribution of the average surface water temperature (°C, (**a**)) and surface salinity (**b**) in the South Sea of Korea in 2018–2022.

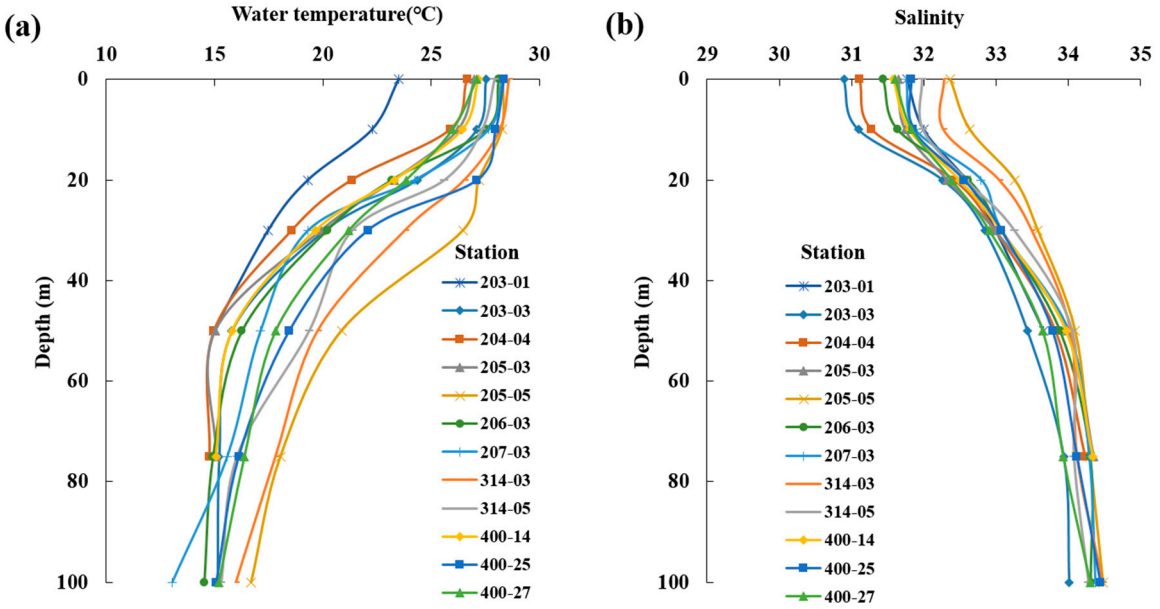

Figure 3. Vertical distribution of the average water temperature (°C, (**a**)) and salinity (**b**) in the South Sea of Korea in 2018–2022.

3.2. Concentrations of Dissolved Inorganic Nutrients

The concentrations of major dissolved inorganic nutrients by depth in the South Sea of Korea are presented in Table 2. During the study period, the average concentration ranges for NH_4, NO_2 + NO_3, PO_4, and SiO_2 were 0.5–1.8 μm, 0.5–12.7 μm, 0.1–1.2 μm, and 2.7–18.1 μm, respectively. No significant differences were observed at the surface level among the sampling stations. Excluding NH_4 levels, vertically, the nutrient concentrations were relatively low in the surface mixed layer (0–30 m depth) but tended to be high below 50 m (one-way analysis of variance, $p < 0.01$). These findings indicate that material exchange was restricted between the surface mixed layer and deeper layers due to the formation of the summer thermocline.

Table 2. Average dissolved inorganic nutrient concentrations by depth (m) studied in the South Sea of Korea during the cruise period (2018–2022).

St.	Depth	NH_4	NO_2 + NO_3	PO_4	SiO_2	St.	Depth	NH_4	NO_2 + NO_3	PO_4	SiO_2
203-01	0	1.0 ± 0.4	1.1 ± 0.9	0.2 ± 0.1	6.3 ± 1.6	207-03	0	1.1 ± 0.6	1.7 ± 2.5	0.2 ± 0.1	6.2 ± 2.2
	10	1.2 ± 0.8	1.8 ± 1.5	0.1 ± 0.1	7.1 ± 2.0		10	0.9 ± 0.5	3.8 ± 7.6	0.2 ± 0.3	8.4 ± 8.6
	20	1.0 ± 0.6	4.4 ± 1.7	0.4 ± 0.2	9.3 ± 1.3		20	1.1 ± 0.5	1.5 ± 1.6	0.4 ± 0.3	5.5 ± 1.9
	30	1.1 ± 0.6	7.6 ± 0.9	0.6 ± 0.3	11.1 ± 1.0		30	0.9 ± 0.4	4.5 ± 3.3	0.5 ± 0.1	9.1 ± 3.3
	50	1.2 ± 0.6	9.3 ± 1.8	0.7 ± 0.3	12.7 ± 1.3		50	1.0 ± 0.6	8.5 ± 1.5	0.6 ± 0.3	14.8 ± 8.4
							75	0.9 ± 0.4	10.7 ± 1.5	0.8 ± 0.4	15.1 ± 2.0
							100	1.0 ± 0.5	12.7 ± 1.6	1.1 ± 0.4	18.1 ± 2.6
203-03	0	0.8 ± 0.3	0.6 ± 0.4	0.2 ± 0.1	5.2 ± 3.0	314-03	0	1.1 ± 0.4	0.7 ± 0.4	0.2 ± 0.1	3.3 ± 2.2
	10	0.7 ± 0.2	2.8 ± 4.8	0.4 ± 0.4	7.7 ± 4.8		10	1.1 ± 0.6	0.6 ± 0.4	0.2 ± 0.2	3.0 ± 2.4
	20	0.9 ± 0.4	4.1 ± 5.0	0.4 ± 0.5	8.9 ± 4.4		20	0.8 ± 0.2	0.6 ± 0.3	0.2 ± 0.2	2.7 ± 0.7
	30	0.7 ± 0.5	4.7 ± 2.6	0.3 ± 0.2	9.2 ± 1.8		30	0.7 ± 0.4	1.3 ± 0.8	0.2 ± 0.1	5.0 ± 1.8
	50	0.6 ± 0.3	9.4 ± 2.1	0.7 ± 0.4	12.6 ± 2.8		50	0.6 ± 0.2	6.9 ± 2.0	0.7 ± 0.7	9.6 ± 3.3
	75	0.8 ± 0.6	7.5 ± 3.8	0.6 ± 0.2	11.1 ± 4.1		75	0.5 ± 0.2	9.5 ± 1.9	0.7 ± 0.3	13.1 ± 1.8
	100	0.8 ± 0.5	8.5 ± 3.3	0.6 ± 0.2	12.3 ± 3.6		100	0.8 ± 0.3	12.4 ± 0.7	1.2 ± 0.6	17.5 ± 1.8
204-03	0	1.2 ± 0.4	1.0 ± 0.4	0.1 ± 0.1	5.9 ± 2.2	314-05	0	0.7 ± 0.2	0.6 ± 0.5	0.2 ± 0.2	4.7 ± 3.3
	10	1.2 ± 0.8	1.6 ± 4.8	0.2 ± 0.2	6.8 ± 2.9		10	1.0 ± 0.5	0.8 ± 0.7	0.2 ± 0.2	4.8 ± 3.5
	20	1.0 ± 0.6	2.7 ± 5.0	0.3 ± 0.2	8.5 ± 2.3		20	0.7 ± 0.2	0.7 ± 0.4	0.3 ± 0.2	5.0 ± 3.2
	30	1.0 ± 0.6	3.7 ± 2.6	0.4 ± 0.3	8.8 ± 2.2		30	0.7 ± 0.2	2.7 ± 2.2	0.3 ± 0.4	6.1 ± 3.4
	50	0.9 ± 0.6	8.1 ± 2.1	0.6 ± 0.2	12.1 ± 3.1		50	0.8 ± 0.3	6.2 ± 2.5	0.6 ± 0.4	9.6 ± 3.6
	75	1.1 ± 0.3	10.4 ± 3.8	0.8 ± 0.3	14.8 ± 5.3		75	0.6 ± 0.3	8.7 ± 2.2	0.8 ± 0.3	12.4 ± 2.8
							100	0.7 ± 0.4	10.9 ± 1.7	1.1 ± 0.4	15.3 ± 3.0
205-03	0	1.0 ± 0.3	0.5 ± 0.1	0.2 ± 0.1	5.8 ± 2.2	400-14	0	0.9 ± 0.5	1.1 ± 1.6	0.3 ± 0.4	5.4 ± 2.8
	10	0.9 ± 0.3	0.6 ± 0.2	0.2 ± 0.2	6.4 ± 2.2		10	0.9 ± 0.7	1.0 ± 1.1	0.3 ± 0.3	5.8 ± 3.6
	20	0.7 ± 0.3	2.6 ± 2.4	0.3 ± 0.2	6.9 ± 3.9		20	1.1 ± 0.9	1.9 ± 2.6	0.3 ± 0.2	6.9 ± 3.9
	30	0.8 ± 0.3	5.4 ± 4.0	0.5 ± 0.2	8.8 ± 4.5		30	0.8 ± 0.3	5.8 ± 2.9	0.5 ± 0.4	9.7 ± 3.0
	50	0.9 ± 0.5	11.2 ± 2.4	0.8 ± 0.2	15.9 ± 2.5		50	0.7 ± 0.6	10.4 ± 1.8	1.1 ± 0.5	15.1 ± 3.5
	75	0.8 ± 0.4	11.7 ± 1.7	1.0 ± 0.2	16.7 ± 2.2		75	0.6 ± 0.4	11.9±1.4	1.0 ± 0.4	17.2 ± 2.0
205-05	0	1.0 ± 0.6	0.6 ± 0.4	0.4 ± 0.5	3.1 ± 1.8	400-25	0	1.2 ± 0.7	0.9 ± 0.6	0.2 ± 0.2	4.5 ± 2.1
	10	0.8 ± 0.3	0.8 ± 0.4	0.2 ± 0.1	3.1 ± 1.5		10	1.0 ± 0.7	1.1 ± 0.8	0.3 ± 0.4	3.6 ± 1.4
	20	1.0 ± 0.6	0.9 ± 0.8	0.4 ± 0.3	2.8 ± 1.4		20	0.9 ± 0.3	1.2 ± 1.1	0.3 ± 0.4	3.8 ± 2.1
	30	0.7 ± 0.3	1.6 ± 1.5	0.3 ± 0.2	6.9 ± 7.3		30	0.8 ± 0.2	4.3 ± 4.6	0.4 ± 0.4	7.2 ± 4.6
	50	0.9 ± 0.4	5.0 ± 3.0	0.3 ± 0.1	7.3 ± 3.7		50	0.6 ± 0.2	7.8 ± 1.6	0.7 ± 0.4	10.5 ± 2.3
	75	0.8 ± 0.3	8.9 ± 2.2	0.7 ± 0.2	11.4 ± 3.4		75	0.5 ± 0.3	10.0 ± 1.7	0.9 ± 0.4	13.7 ± 2.1
	100	0.8 ± 0.4	10.7 ± 1.5	0.8 ± 0.2	14.4 ± 1.8		100	1.0 ± 0.4	12.4 ± 1.1	1.1 ± 0.4	17.4 ± 1.1
206-03	0	1.0 ± 0.4	0.6 ± 0.3	0.3 ± 0.4	4.9 ± 2.3	400-27	0	0.7 ± 0.3	0.9 ± 0.3	0.3 ± 0.3	6.1 ± 1.8
	10	0.9 ± 0.3	0.5 ± 0.3	0.2 ± 0.1	5.4 ± 2.5		10	1.1 ± 0.6	0.6±0.3	0.2 ± 0.3	6.2 ± 2.2
	20	0.9 ± 0.3	1.2 ± 1.2	0.2 ± 0.1	6.4 ± 2.2		20	0.8 ± 0.5	1.2 ± 0.8	0.4 ± 0.3	6.8 ± 1.0
	30	0.9 ± 0.3	3.5 ± 3.4	0.3 ± 0.1	8.7 ± 1.9		30	0.8 ± 0.5	3.1 ± 2.3	0.4 ± 0.3	7.9 ± 1.8
	50	1.8 ± 1.9	8.2 ± 3.8	0.6 ± 0.4	12.6 ± 4.6		50	1.5 ± 1.5	7.6 ± 1.5	0.7 ± 0.4	11.1 ± 1.4
	75	0.8 ± 0.3	8.4 ± 5.8	0.8 ± 0.3	14.0 ± 5.9		75	0.7 ± 0.4	9.3 ± 1.5	0.8 ± 0.4	12.8 ± 1.4
	100	0.9 ± 0.3	11.3 ± 3.0	0.9 ± 0.2	16.5 ± 4.9		100	0.8 ± 0.8	11.3 ± 2.4	1.0 ± 0.4	15.9 ± 3.0

3.3. Phytoplankton Abundances and Dominant Species

The average phytoplankton abundance during the summer ranged from 180,428 to 2,140,800 cells·L^{-1}, with an overall of 879,231 ± 931,391 cells·L^{-1}. Spatially, the western areas (203 and 204 transect) showed 3–5 times higher abundances than the eastern areas (206 and 207 transect). Vertically, approximately 91% of the total phytoplankton abundance was observed in the surface mixed layer (0–30 m depth) due to summer stratification, indicating a significant difference in the phytoplankton abundance between the surface and deeper layers. Nanoflagellates predominated the survey period (<20 μm), with *Chaetoceros curvisetus*, *Dactyliosolen fragilissimus*, and *Skeletonema costatum*. representing the dominant species at different sampling points (Table 3).

Table 3. Dominant phytoplankton species rankings in the South Sea of Korea in 2018–2022.

	2018	2019	2020	2021	2022
First	Nanoflagellates (<20 μm; 62.0%)	Nanoflagellates (<20 μm; 68.8%)	Nanoflagellates (<20 μm; 77.5%)	Nanoflagellates (<20 μm; 29.3%)	Nanoflagellates (<20 μm; 90.0%)
Second	*Pseudo-nitzschia* spp. (13.2%)	*Chaetoceros curvisetus*. (19.7%)		*Dactyliosolen fragilissimus* (25.2%)	
Third				*Skeletonema* spp. (7.6%)	

3.4. Contributions of Size-Fractionated Chl-a Concentrations

The average surface concentration of chl-*a* in the South Sea of Korea in August ranged from 0.15 to 1.24 μg·L^{-1}, with an overall average of 0.33 ± 0.30 μg·L^{-1}. A significantly higher concentration was observed at station 203-01, whereas no significant differences were observed at the other stations (Figure 4a). The vertical distribution of the chl-*a* concentration ranged from 0.06 to 1.90 μg·L^{-1}, with an overall average of 0.43 ± 0.32 μg·L^{-1}. The subsurface chlorophyll-*a* maximum (SCM) layer developed at depths ranging from 10 to 50 m depending on the station (Figure 4b). The SCM layer formed according to the depth of the thermocline at each station, and the chl-*a* concentration generally decreased from the surface mixed layer to the deeper layers.

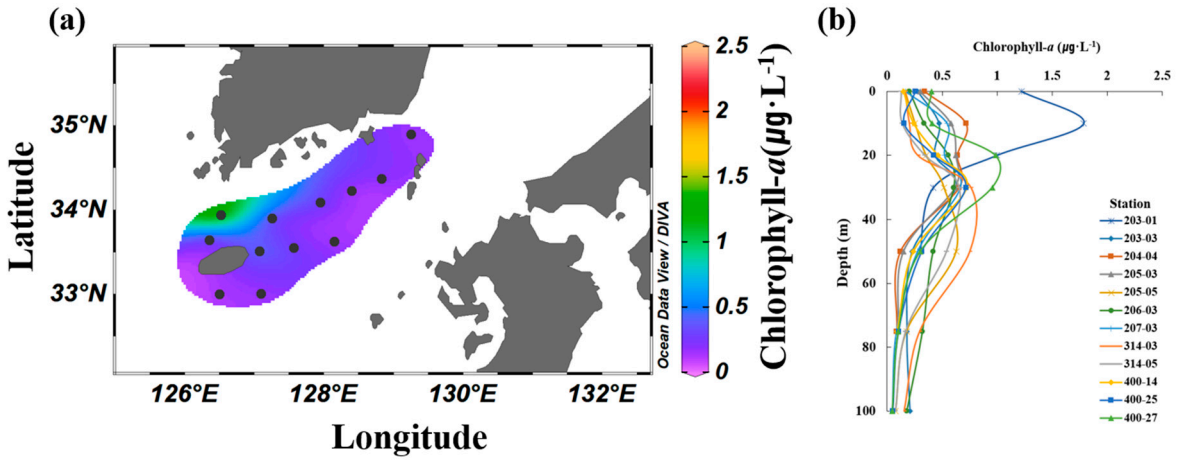

Figure 4. Average spatial (**a**) and vertical (**b**) distributions of Chl-*a* (μg L^{-1}) in the South Sea of Korea from 2018 to 2021.

The contributions of different phytoplankton to the chl-*a* concentration are presented in Table 4 according to size. The average contribution rates for the micro, nano, and pico classes were 6.3–37.9% (16.7 ± 6.5%), 9.3–59.9% (23.2 ± 11.7%), and 26.6–79.6% (60.1 ± 12.6%), respectively. Picophytoplankton were the most abundant summer phytoplankton in the South Sea of Korea. The spatial distribution characteristics based on the SI revealed that smaller phytoplankton formed major clusters at all surveyed stations, with the lowest SI values (<8) observed at stations 206-03 and 314-05 (Figure 5).

Table 4. Average chl-*a* composition in phytoplankton of different sizes (M, N, and P) at each depth (m) in the South Sea of Korea during the cruise period (2018–2021).

		Chl-*a* Composition (%)					Chl-*a* Composition (%)		
St.	**Depth**	**M**	**N**	**P**	**St.**	**Depth**	**M**	**N**	**P**
203-01	0	21.1 ± 10.2	39.0 ± 35.1	39.9 ± 30.4	207-03	0	19.0 ± 9.0	29.2 ± 36.7	51.8 ± 30.8
	10	19.9 ± 13.2	21.7 ± 7.7	58.4 ± 16.9		10	37.2 ± 37.3	9.3 ± 5.3	53.5 ± 32.2
	20	23.0 ± 18.2	23.4 ± 8.1	53.8 ± 20.9		20	7.8 ± 10.8	14.1 ± 11.0	78.1 ± 13.8
	30	21.9 ± 12.9	28.2 ± 7.3	49.9 ± 11.6		30	30.4 ± 28.0	11.2 ± 6.8	58.4± 24.8
	50	14.8 ± 15.0	31.6 ± 11.2	53.5 ± 23.1		50	10.1 ± 6.8	24.4 ± 9.5	65.4 ± 10.8
						75	26.0 ± 17.7	35.8 ± 15.7	38.2 ± 32.6
						100	25.6 ± 16.2	41.0 ± 9.4	33.4 ± 22.1
203-03	0	19.9 ± 25.6	25.7 ± 17.7	54.4 ± 32.2	314-03	0	17.2 ± 16.9	20.3 ± 24.2	62.5 ± 17.1
	10	17.8 ± 22.2	19.4 ± 7.6	62.8 ± 17.3		10	13.8 ± 12.3	14.8 ± 7.9	71.4 ± 8.6
	20	18.2 ± 19.7	16.4 ± 4.3	65.4 ± 17.1		20	15.6 ± 7.1	14.3 ± 5.1	70.1 ± 9.4
	30	16.2 ± 9.0	20.6 ± 7.3	63.3 ± 13.2		30	27.9 ± 23.7	14.9 ± 3.3	57.2 ± 25.5
	50	9.0 ± 7.0	33.3 ± 2.3	57.7 ± 8.3		50	26.9 ± 27.7	18.8 ± 1.8	54.4 ± 29.0
	75	12.1 ± 10.3	42.2 ± 13.2	45.7 ± 6.8		75	11.1 ± 12.4	34.5 ± 23.8	54.3 ± 19.4
	100	14.3 ± 11.5	46.6 ± 16.3	39.1 ± 9.4		100	14.7 ± 16.3	31.8 ± 4.2	53.5 ± 13.5
204-04	0	22.5 ± 25.6	14.1 ± 3.5	63.4 ± 14.0	314-05	0	15.9 ± 6.5	22.9 ± 19.8	61.3 ± 21.6
	10	16.5 ± 22.2	18.4 ± 9.4	65.0 ± 13.0		10	14.2 ± 6.6	13.7 ± 6.2	72.1 ± 9.0
	20	12.5 ± 19.7	15.5 ± 6.2	72.0 ± 7.1		20	7.3 ± 5.6	23.1 ± 7.7	79.6 ± 2.4
	30	13.7 ± 9.0	22.3 ± 8.4	64.0 ± 11.5		30	12.2 ± 10.8	14.5 ± 9.8	73.3 ± 9.9
	50	17.9 ± 7.0	38.9 ± 6.5	43.2 ± 10.4		50	19.0 ± 15.3	17.4 ± 4.3	63.6 ± 18.6
	75	20.0 ± 10.3	40.4 ± 8.6	39.6 ± 4.1		75	11.6 ± 9.2	30.1 ± 7.5	58.3 ± 3.1
						100	14.6 ± 5.7	41.0 ± 7.2	44.4 ± 7.8
205-03	0	21.2 ± 18.0	12.5 ± 4.9	66.3 ± 14.0	400-14	0	13.4 ± 15.4	19.3 ± 21.1	67.3 ± 17.6
	10	22.3 ± 20.4	11.9 ± 4.1	65.8 ± 19.9		10	21.3 ± 12.2	11.5 ± 6.9	67.3 ± 9.5
	20	19.1 ± 17.1	18.1 ± 9.6	62.8 ± 8.2		20	14.2 ± 13.1	11.8 ± 7.7	74.0 ± 7.5
	30	22.7 ± 11.2	17.4 ± 11.1	59.8 ± 12.6		30	14.8 ± 10.1	16.3 ± 9.3	69.0 ± 11.5
	50	20.9 ± 16.1	36.1 ± 7.3	43.0 ± 10.4		50	10.5 ± 12.8	30.6 ± 7.2	58.9 ± 12.2
	75	24.0 ± 2.8	41.7 ± 8.4	34.3 ± 7.8		75	10.6 ± 12.5	39.8 ± 5.1	49.5 ± 7.9
205-05	0	18.9 ± 5.7	14.0 ± 4.6	67.1 ± 1.4	400-25	0	37.9 ± 35.2	10.8 ± 4.4	51.3 ± 31.3
	10	12.7 ± 9.0	11.9 ± 3.8	75.4 ± 5.5		10	28.9 ± 5.0	12.9 ± 2.7	58.2 ± 3.9
	20	7.8 ± 5.2	13.4 ± 5.7	78.8 ± 3.8		20	24.0 ± 14.4	14.7 ± 2.8	61.3 ± 12.1
	30	9.8 ± 2.1	19.2 ± 9.6	71.0 ± 10.9		30	13.2 ± 4.0	14.2 ± 6.0	72.6 ± 8.5
	50	24.1 ± 36.8	12.8 ± 9.0	63.1 ± 29.2		50	17.2 ± 11.2	15.5 ± 3.8	67.3 ± 7.9
	75	15.4 ± 15.4	21.0 ± 9.4	63.7 ± 23.5		75	8.6 ± 11.5	24.8 ± 6.9	66.6 ± 17.5
	100	18.0 ± 11.5	29.2 ± 13.7	52.8 ± 18.7		100	16.0 ± 14.9	57.4 ± 31.9	26.6 ± 21.9
206-03	0	9.4 ± 12.5	14.1 ± 3.1	76.5 ± 11.5	400-27	0	11.7 ± 11.3	10.1 ± 1.7	78.3 ± 12.9
	10	12.9 ± 14.8	12.5 ± 2.1	74.6 ± 15.1		10	18.1 ± 27.3	12.2 ± 3.7	69.7 ± 30.4
	20	12.1 ± 12.2	10.3 ± 2.1	77.6 ± 11.3		20	9.1 ± 118	12.9 ± 4.0	78.0 ± 12.5
	30	6.3 ± 6.5	14.3 ± 4.2	79.4 ± 9.6		30	10.4 ± 12.8	24.7 ± 10.0	64.9 ± 4.3
	50	11.2 ± 10.9	25.9 ± 5.4	62.9 ± 16.0		50	13.8 ± 10.3	21.3 ± 2.0	64.8 ± 9.0
	75	12.2 ± 13.3	37.0 ± 15.6	50.8 ± 11.2		75	9.9 ± 5.7	30.3 ± 10.7	59.9 ± 6.7
	100	13.2 ± 11.8	59.9 ± 15.2	26.9 ± 14.7		100	11.9 ± 11.6	45.4 ± 13.2	42.6 ± 3.3

Note(s): M: micro size (>20 μm); N: nano size (20 μm ≥ chl-*a* ≥ 3 μm); P: pico size (<3 μm)

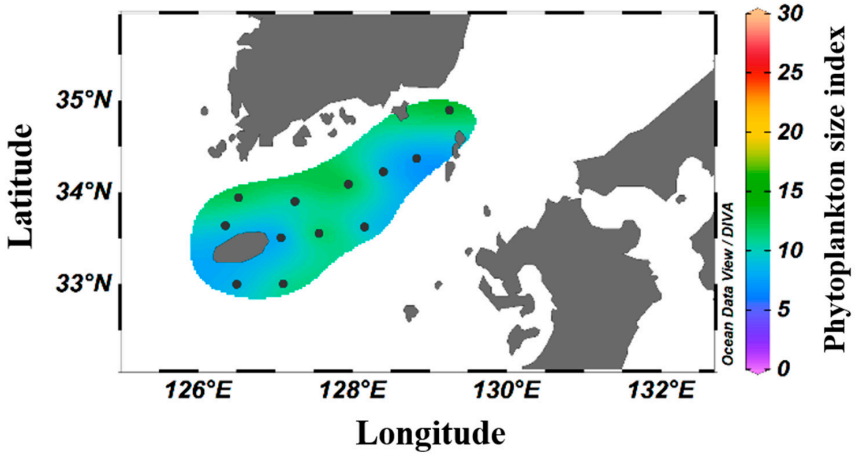

Figure 5. Spatial distribution of the average phytoplankton SI in the South Sea of Korea in 2018–2021.

4. Discussion

According to the IPCC comprehensive report published in 2023, the global warming trend is accelerating. Although the AR5 indicated a 0.85 °C increase in the global surface temperature since the Industrial Revolution, the most recent AR6 indicated a larger increase of approximately 1.1 °C [1]. During the 55 years from 1968 to 2022, the annual average surface water temperature in Korean waters increased at a rate of 0.0248 °C·yr^{-1}, resulting in a total increase of approximately 1.36 °C. During the same period, the annual average global surface water temperature rose at 0.0094 °C·yr^{-1}, leading to an increase of approximately 0.52 °C. These data suggest that the temperature of Korean waters is increasing approximately 2.5 times faster than the global average [19]. Focusing on the 55 summers from 1968 to 2022, the annual average surface water temperature in Korean waters increased at a rate of 0.0261 °C·yr^{-1}, reaching approximately 1.44 °C. Regarding the waters of the South Sea of Korea, the average annual summer surface water temperature increased at 0.0211 °C·yr^{-1}, resulting in an increase of approximately 1.16 °C. These data indicate a strong increasing trend in surface water temperatures (Figure 6). Additionally, the long-term trends over the 55 years regarding temperature differences between the surface and deeper layers (depths of 75–100 m) revealed an annual increase of 0.02 °C. These findings suggest that stratification around the surface layer in the South Sea of Korea is gradually intensifying.

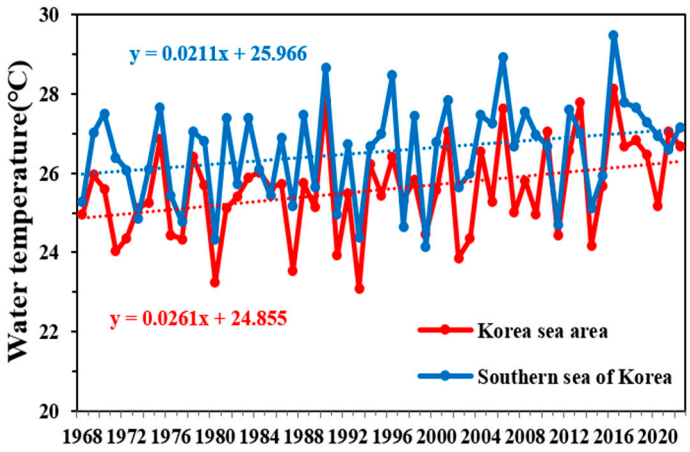

Figure 6. Temporal variations in the annual mean surface water temperature in the Korean sea area and South Sea of Korea from 1968 to 2022 in the summer, according to Korea Oceanographic Data Center (KODC) data.

In the Korean waters around Ulleungdo and Dokdo, the surface nutrient concentrations during the spring increase following strong winds that induce vertical mixing rather than after stratification. This phenomenon has been reported as a key driver of phytoplankton blooms [38]. Moreover, the nutrient levels in the Gulf of Mexico increased following Hurricane Katrina, with vertical mixing playing a significant role in promoting phytoplankton blooms [39]. Conversely, the intensification of stratification can reduce the material exchange between the surface layer and deeper layers, implying a potential limitation in the supply of nutrients to the surface layer. The long-term nutrient variations (1990–2022) within the surface mixed layer (depths of 0–20 m) in the South Sea of Korea revealed a decreasing trend for all observed nutrients, including nitrites, nitrates, phosphates, and silicates. This suggests that nutrient influx from the deeper layers is decreasing due to increased stratification (Figure 7). This decline in nutrient influx could act as a significant limiting factor for the growth of phytoplankton, which exhibit high abundance within the surface mixed layer [40–43].

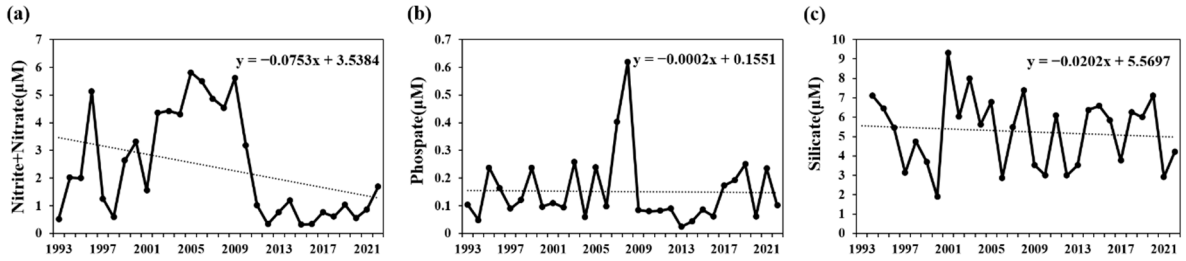

Figure 7. Temporal variations in the annual mean nutrients in the surface mixed layer (0–20 m) of the South Sea of Korea from 1993 to 2022 in summer, according to KODC data. (**a**) Nitrites + nitrates, (**b**) phosphates, and (**c**) silicates.

Findings from previous research related to phytoplankton community structures in the South Sea of Korea during the summer season showed that the diatom *Chaetoceros affinis* (dominance rate: 75%) was the dominant species [24]. The dinoflagellates *Prorocentrum triestinum* (22.3%) and *Scrippsiella trochoidea* (19.7%) were the first- and second-most dominant species, and the diatoms *Leptocylindrus mediterraneus* (11.6%), *Skeletonema costatum* (5.5%), and *Dactyliosolen fragilissimus* (5.2%) appeared as subdominant species [44]. Other reports showed that diatoms such as *Chaetoceros* spp. (about 20–30%) and *Cylindrotheca closterium* (18.7%) and *Pseudo-nitzschia delicatissima*, as well as dinoflagellates *Gyrodinium* spp. (about 10–16%) and *Gyrodinium* spp. (about 4–10%) predominated [27,29,30]. The occurrence rate of the phytoplankton dominant group was reported to be about 10–35% for diatoms, about 10–18% for dinoflagellates, and about 2–16% for nanoflagellates [30]. Notably, dominant phytoplankton species previously reported in the South Sea of Korea are larger than micro-scale. In contrast, comparing the past micro-sized plant plankton dominant species with the average occurrence rate investigated this time (2018–2022), among diatoms, *Chaetoceros* spp. 1.7%, *Cylindrotheca closterium* 1.3%, *Dactyliosolen fragilissimus* 5.3%, and *Skeletonema costatum* 2.0%. Among dinoflagellates, *Gymnodinium* spp. 1.6%, *Gyrodinium* spp. 0.6%, *Prorocentrum triestinum* 0.1%, and *Scrippsiella trochoidea* 0.2% appeared. By phytoplankton group, diatoms 4.5–66.7% (average 29.2%), dinoflagellates 3.7–6.9 (average 4.9%), and nanoflagellates 29.3–90.0% (average 65.5), respectively. The results showed an increasing trend in the appearance of smaller species in the South Sea of Korea, which was considered to be due to decreased nutrient levels.

Justic et al. [42] reported that if the N: P ratio is <10.0 and the Si: N is >1.0, N acts as a limiting factor for phytoplankton growth; whereas if the N: P ratio is >22.0 and Si: P ratio is >22.0, P serves as the limiting factor; if the Si: P ratio is <10.0 and the Si: N ratio is <1.0, Si represents the limiting factor. In this survey, the average N: P ratio was 19.1, Si: N ratio was 2.4, and Si: P ratio was 42.3. Although no single nutrient acted as a limiting factor, the nutrient concentrations in the surface mixed layer remained low (<0.2 μM), excluding select periods. Dortch and Whitledge [41] reported that the threshold nutrient concentrations limiting phytoplankton growth were a DIN of 1.0 μm, phosphate concentration of 0.2 μm, and silicate concentration of 2.0 μm. However, phosphate serves as an important limiting factor for diatom growth, more so than for flagellates [45]. In fact, even when nitrate levels exceed the growth-limiting threshold, phytoplankton do not utilize nitrate if phosphate is insufficient, inhibiting their growth [46]. These findings suggest that the dominance of flagellates <20 μm in the phytoplankton community of the South Sea of Korea during the summer months was likely due to these nutrient dynamics. During this survey period, the average size distribution was 16.7% for micro-sized phytoplankton, 23.2% for nano-sized, and 60.1% for pico-sized. The pico-sized phytoplankton showed a high chl-*a* contribution, particularly in the surface mixed layer (0–20 m), higher than that reported by studies of other Korean waters (Table 5). Previous studies showed that in the East/Japan Sea regions of the Uljin, Chuksan, and Ulsan coasts, the proportion of micro-sized phytoplankton was either higher than or similar to the combined proportions of nano- and pico-sized phytoplankton [45–49]. In the eastern Yellow Sea, small phytoplankton with sizes below

20 µm accounted for an average of 74% of all chl-*a* production [21]. In contrast, in this study, high contributions were made by nano- and pico-sized phytoplankton across all depths, particularly in the surface mixed layer where nutrient levels were relatively low. These results are consistent with recent results reported for the East/Japan Sea and East China Sea, which revealed that rising surface water temperature strengthens stratification and reduces nutrient influx into the surface mixed layer, resulting in a high chl-*a* contribution from smaller phytoplankton [15,16]. The statistical analyses indicated that the correlation between nutrient levels and phytoplankton size structure was clear. The RDA results related to chl-*a* and environmental factors showed that as the depth increased, the nutrient concentration tended to increase as a function of the phytoplankton size. These findings likely resulted from limited nutrient influx to the surface due to increased stratification. Meanwhile, nanophytoplankton showed a higher chl-*a* contribution rate in layers with higher nutrient levels. In contrast, picophytoplankton displayed negative correlations with all nutrients except NH_4, indicating that they had a higher chl-*a* contribution rate when nutrient levels were low (Figure 8).

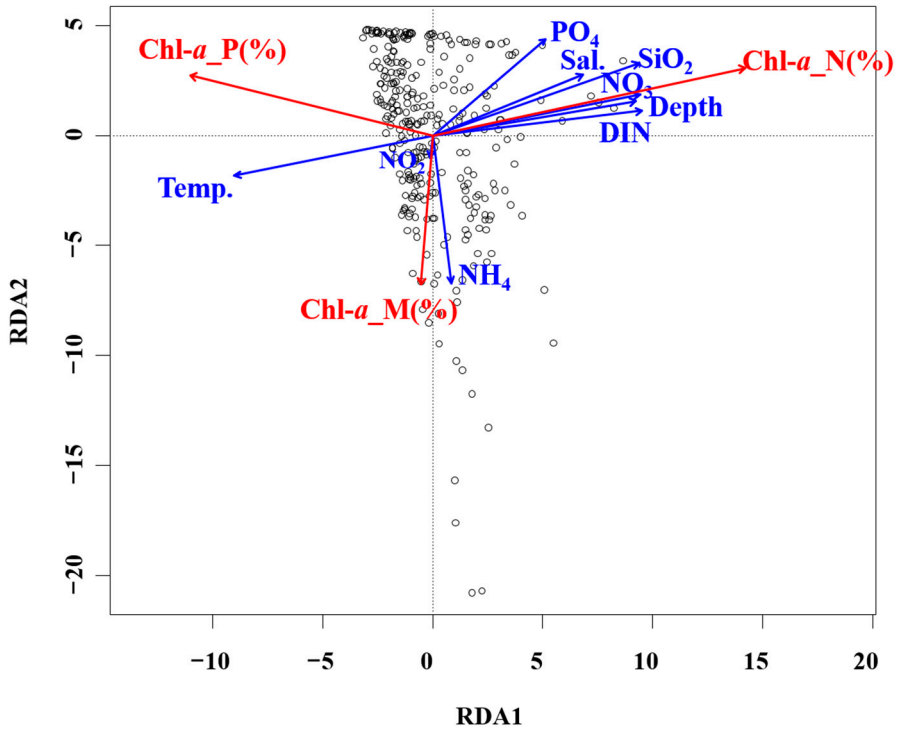

Figure 8. RDA ordination plots showing relationships between environmental and biological conditions in the South Sea of Korea. Temp., temperature; Sal., salinity.

Similar results are frequently observed in other sea areas. In the Mediterranean Sea, both direct observations and satellite data have shown that picophytoplankton <2 µm contribute an average of 31–92%, depending on the season. Low nitrogen and phosphorus levels were reported as the primary causes of these observations [50]. In Blanes Bay of the Mediterranean Sea, high temperatures and nutrient deficiency were reported as the main causes of the picophytoplankton predominance [51]. In the summer and winter in the central Tyrrhenian Sea, and during the spring in the eastern Levantine Basin in the Mediterranean, picophytoplankton comprised 44–90% and 54–64% of the community, respectively [52,53]. Recent satellite data also revealed that the summer phytoplankton in Japan's Yamato Basin and the Japan Basin were composed of >50% picophytoplankton [54]. Son et al. [55] reported that while the contribution of micro-sized phytoplankton to chl-*a* levels rapidly decreased, those of nano- and pico-sized phytoplankton increased in the northern East China Sea. High compositions of nano- and pico-sized phytoplankton have

been reported in various other sea areas [56–61]. A common characteristic of these sea areas is that they are oligotrophic. In nutrient-deficient waters, smaller phytoplankton have a larger surface area per unit volume, allowing for quicker nutrient exchange through the cell surface, leading to smaller phytoplankton predominance [62–64].

Table 5. Size fractionation of phytoplankton observed in the different coastal waters of Korea and global ocean areas.

		Relative Ratio (%)			
Area	**Date**	**Pico Size**	**Nano Size**	**Micro Size**	**References**
Uljin coast	2003–2004/ April		33.9	66.1	[47]
Chuksan coast	2000–2002/ seasonal		58.4	41.6	[48]
Ulsan port and coast	2007–2009/ seasonal	22.4–38.2	58.2–74.5	3.9–81.2 (52.3)	[49]
Northern East China Sea	2018–2020/ August	45.6	31.2	23.2	[15]
East Sea	2018–2020/ August	45.9	33.5	20.6	[16]
Mediterranean Sea		31–92			[50]
Adriatic Sea (North)	1986 and 1988/August, 1987/July			10–23	[58]
Levantine Basin	1992/March	54.3–64.2			[52]
Blanes Bay	1997/summer	>50			[51]
Atlantic Meridional Transect (Oligotrophic)	1996/April, October 1997/April, October	80	16	4	[59]
Algerian Basin	1996/October	42–62	38–58		[60]
South China Sea	1998/summer	63	22	16	[61]
Tyrrhenian Sea (South)	2005/July	44–81			[53]
Japan Basin Yamato Basin	2010/July	56 56			[54]
South Sea of Korea	2018–2021/summer	60.1	23.2	16.7	**This study**

Note(s): Values shown in parentheses indicate mean values.

Phytoplankton miniaturization can reduce the primary productivity of marine ecosystems [17,65]. Joo et al. [17] reported that the primary productivity in the East Sea measured using the moderate resolution imaging spectroradiometer decreased by 13% per decade as the abundances of picophytoplankton < 2 μm increased. In the Amundsen Sea, a strong negative correlation was observed between the predominance of phytoplankton < 5 μm and the total primary productivity, which was attributed to the lower carbon uptake rates of smaller phytoplankton [63]. Although direct research on the primary productivity in the South Sea has been scarce, previous research results from nearby waters reported by Gong et al. [66] and Zhang et al. [67] revealed summer primary productivities in the East China Sea of 714 mg $C \cdot m^{-2} \cdot d^{-1}$ and 414 mg $C \cdot m^{-2} \cdot d^{-1}$, respectively. In the East Sea, these values ranged from 353 to 716 mg $C \cdot m^{-2} \cdot d^{-1}$ [18,68,69], while in the Yellow Sea, the productivity ranged from 291 to 649 mg $C \cdot m^{-2} \cdot d^{-1}$ [14,70,71]. In contrast, the results of this study revealed a summer average of 227 mg $C \cdot m^{-2} \cdot day^{-1}$ (unpublished data), indicating that the primary productivity observed in this study was lower than that reported previously. Phytoplankton miniaturization was considered the cause of these differences. Richardson [72] predicted that climate change-induced stratification and the subsequent decrease in surface

nutrients would increase the picophytoplankton abundance, resulting in the dominance of medium-sized zooplankton (microzooplankton; <200 μm) and gelatinous zooplankton (salps, doliolids, and ctenophores), along with a decrease in their biomass. Moreover, medium-sized zooplankton do not directly consume picophytoplankton but rather feed on ciliates that have consumed picophytoplankton [73,74]. However, the net growth efficiency of medium-sized zooplankton that consume ciliates is only ~13%, indicating a relatively low energy efficiency [75]. Consequently, the increase in water temperature due to climate change likely strengthened stratification, reducing the inflow of nutrients from the bottom layer to the surface, leading to phytoplankton miniaturization within the surface mixed layer (Figure 9). Accordingly, small, low-productivity phytoplankton are thought to be less efficient at transferring carbon to consumers at higher trophic levels, negatively impacting overall ocean productivity.

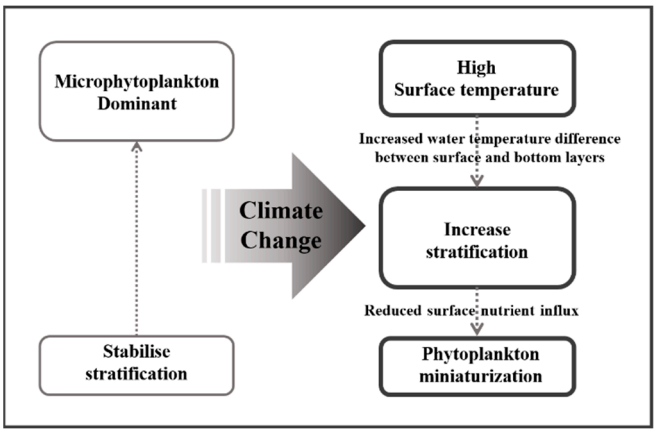

Figure 9. Schematic diagram of phytoplankton effects due to climate change.

5. Summary

To investigate the effects of climate change on the summer phytoplankton community structure in the South Sea of Korea and its potential impact on marine ecosystems, we analyzed previous physical and chemical data from the KODC for the South Sea of Korea. Additionally, we conducted stratified field surveys at 12 stations in August from 2018 to 2022. The results indicate that the increase in the surface water temperature due to climate change has led to significant stratification, resulting in lower nutrient concentrations within the surface mixed layer. Consequently, the phytoplankton community structure was dominated by flagellates <20 μm throughout the survey period, excluding select stations at certain periods. We also observed increased abundances of nano- and pico-size phytoplankton in the South Sea of Korea compared to previous levels. An analysis of chl-*a* concentrations revealed that picophytoplankton contributed 60.1% to the overall chl-*a* concentration in the phytoplankton community, which is higher than the contributions observed in other sea areas during the summer. These findings confirm that the phytoplankton miniaturization trend has been recently intensifying in the South Sea. Our RDA indicate that the high chl-*a* contribution of picophytoplankton had a strong negative correlation with nutrient levels, suggesting that phytoplankton miniaturization was exacerbated by the low nutrient levels in the surface mixed layer. Thus, phytoplankton miniaturization reduces primary productivity and leads to the formation of more complex microbial food webs rather than simple food webs. In conclusion, the South Sea of Korea is experiencing intensified phytoplankton miniaturization, which is expected to reduce the primary productivity and increase the complexity of the food web. Such effects could reduce the energy-transfer efficiency to consumers higher up in the food chain, causing an overall decline in marine productivity.

Author Contributions: Conceptualization, K.-W.P. and S.-H.Y.; Methodology, K.-W.P. and M.-H.Y.; Validation, K.-W.P.; Formal analysis, K.-W.P. and M.-H.C.; Investigation, K.-W.P., M.-H.Y., K.-S.O., K.-Y.K. and T.-G.P.; Data curation, K.-W.P. and M.-H.C.; Writing—original draft, K.-W.P.; Writing—review & editing, K.-W.P. and S.-H.Y.; Visualization, K.-W.P.; Project administration, K.-Y.K., T.-G.P. and S.-H.Y.; Funding acquisition, S.-H.Y. All authors have read and agreed to the published version of the manuscript.

Funding: This research was supported by the "Countermeasure study of harmful organisms to fisheries damages (R2023038)" funded by the National Institute of Fisheries Science (NIFS), Korea.

Data Availability Statement: No new data were created or analyzed in this study. Data sharing is not applicable to this article.

Acknowledgments: We appreciate the captains and crew of *R/V Tamgu 8* for their assistance with collecting our samples. We would also like to thank the researchers for their assistance with sample analysis.

Conflicts of Interest: The authors declare no conflict of interest.

References

1. IPCC (Intergovernmental Panel on Climate Change). *Climate Change 2023: Synthesis Report. Contribution of Working Group I, II and III to the Sixth Assessment Report of the Intergovernmental Panel on Climate Change*; IPCC: Geneva, Switzerland, 2023; pp. 1–34.
2. IPCC (Intergovernmental Panel on Climate Change). *The Ocean and Cryosphere in a Changing Climate: A Special Report of the IPCC*; Cambridge University Press: Cambridge, UK, 2019; p. 738.
3. IPCC (Intergovernmental Panel on Climate Change). *Climate Change 2022: Impact, Adaptation and Vulnerability. Contribution of Working Group II to the Sixth Assessment Report of the Intergovernmental Panel on Climate Change*; IPCC: Geneva, Switzerland, 2022; pp. 673–816.
4. WMO (World Meteorological Organization). *State of the Global Climate 2021*; WMO No. 1290; WHO: Geneva, Switzerland, 2022; p. 54. Available online: https://wedocs.unep.org/20.500.11822/40033 (accessed on 5 July 2023.).
5. Tont, S.A. Short-period Climatic Fluctuations: Effects on Diatom Biomass. *Science* **1976**, *194*, 942–944. [CrossRef] [PubMed]
6. Venrick, E.L.; McGowan, J.A.; Cayan, D.R.; Hayward, T.L. Climate and Chlorophyll a: Long-term Trends in the Central North Pacific Ocean. *Science* **1987**, *238*, 70–72. [CrossRef] [PubMed]
7. Smayda, T.J. Biogeographical meaning indicators. In *Phytoplankton Manual*; Sournia, A., Ed.; United Nations Educational, Scientific, and Cultural Organization: Paris, France, 1978; pp. 225–229.
8. Yanagi, T. Water, salt, phosphorus and nitrogen budgets of the Japan Sea. *J. Oceanogr.* **2002**, *58*, 797–804. [CrossRef]
9. Onitsuka, G.; Yanagi, T.; Yoon, J.H. A numerical study on nutrient sources in the surface layer of the Japan Sea using a coupled physical-ecosystem model. *J. Geophys. Res.* **2007**, *112*, C05042. [CrossRef]
10. Morimoto, A.; Takikawa, T.; Onitsuka, G.; Watanabe, A.; Moku, M.; Yanagi, T. Seasonal variation of horizontal material transport through the eastern channel of the Tsushima Straits. *J. Oceanogr.* **2009**, *65*, 61–71. [CrossRef]
11. Yoon, Y.H. Spatio-temporal Distributions of Phytoplankton Community in the Coastal Waters of Central South Sea (CWoCSS), Korea. *J. Korean Acad. Coop. Ind. Soc.* **2017**, *18*, 441–453.
12. Han, I.S.; Kee, J.S.; Jung, H.K. Long-term pattern changes of sea surface temperature during summer and winter due to climate change in the Korea Waters. *Fish Aqua Sci.* **2023**, accepted.
13. Park, S.J.; Kim, G.B.; Kwon, H.K.; Han, I.S. Long-term changes in the marginal seas (Yellow Sea, East China Sea, and East/Japan Sea) neighboring the Korean Peninsula. *Mar. Pollut. Bull.* **2023**, *192*, 115012. [CrossRef]
14. Lee, Y.J. Phytoplankton Dynamics and Primary Production in the Yellow Sea during Winter and Summer. Ph.D. Thesis, Inha University, Incheon, Republic of Korea, 2012.
15. Park, K.W.; Oh, H.J.; Moon, S.Y.; Yoo, M.H.; Youn, S.H. Effects of Miniaturization of the Summer Phytoplankton Community on the Marine Ecosystem in the Northern East China Sea. *J. Mar. Sci. Eng.* **2022**, *10*, 315. [CrossRef]
16. Park, K.W.; Oh, H.J.; Hwang, J.D.; Moon, S.Y.; Lee, M.U.; Youn, S.H. Changes in Phytoplankton Size Structure in the East Sea 2018–2020 due to Marine Environment Change. *Korean J. Environ. Biol.* **2022**, *40*, 54–69. [CrossRef]
17. Joo, H.T.; Son, S.H.; Park, J.W.; Kang, J.J.; Jeong, J.Y.; Lee, C.I.; Kang, C.K.; Lee, S.H. Long-term pattern of primary productivity in the East/Japan Sea based on ocean color data derived from MODIS-aqua. *Remote Sens.* **2016**, *8*, 25. [CrossRef]
18. Joo, H.T.; Son, S.H.; Park, J.W.; Kang, J.J.; Jeong, J.Y.; Kwon, J., II; Kang, C.K.; Lee, S.H. Small phytoplankton contribution to the total primary production in the highly productive Ulleung Basin in the East/Japan Sea. *Deep Sea Res. 2 Top. Stud. Oceanogr.* **2017**, *143*, 54–61. [CrossRef]
19. NIFS (National Institute of Fisheries Science). *Annual Report for Climate Change Trends in Fisheries, 2022*; NIFS: Busan, Republic of Korea, 2023; p. 87.
20. Bhavya, P.S.; Kang, J.J.; Jang, H.K.; Joo, H.T.; Lee, J.H.; Lee, J.H.; Park, J.W.; Kim, K.W.; Kim, H.C.; Lee, S.H. The Contribution of Small Phytoplankton Communities to the Total Dissolved Inorganic Nitrogen Assimilation Rates in the East/Japan Sea: An Experimental Evaluation. *J. Mar. Sci. Eng.* **2020**, *8*, 854. [CrossRef]

21. Kim, Y.J.; Youn, S.H.; Oh, H.J.; Kang, J.J.; Lee, J.H.; Lee, D.B.; Kim, K.W.; Jang, H.K.; Kee, J.B.; Lee, S.H. Spatiotemporal Variation in Phytoplankton Community Driven by Environmental Factors in the Northern East China Sea. *Water* **2020**, *12*, 2695. [CrossRef]
22. Kang, J.J.; Jang, H.K.; Lim, J.H.; Lee, D.B.; Lee, J.H.; Bae, H.J.; Lee, C.H.; Kang, C.K.; Lee, S.H. Characteristics of Different Size Phytoplankton for Primary Production and Biochemical Compositions in the Western East/Japan Sea. *Front. Microbiol.* **2020**, *11*, 560102. [CrossRef]
23. Lee, H.W.; Noh, J.H.; Choi, D.H.; Yun, M.S.; Bhavya, P.S.; Kang, J.J.; Lee, J.H.; Kim, K.W.; Jang, H.K.; Lee, S.H. Picocyanobacterial Contribution to The Total Primary Production in the Northwestern Pacific Ocean. *Water* **2021**, *13*, 1610. [CrossRef]
24. Park, J.S.; Lee, S.G. Distribution and Species Composition of Phytoplankton in the Southern Waters of Korea and their Relation to the Character of Water Masses. *Bull. Korean Fish. Soc.* **1990**, *23*, 208–214.
25. Yoon, Y.H.; Kim, S.A. Seasonal variations of phytoplankton population and primary productivity in the southern coastal waters of Korea. 1. A characteristics of the distribution of chlorophyll a and water quality in the dry season in the Yeosuhae Bay and adjoining sea. *J. Korean Environ. Sci. Soc.* **1996**, *5*, 347–359.
26. Lee, Y.S. An influence of inflowing freshwater on the diatom blooms in the eastern coast of Dolsan, Yosu, Korea. *J. Korean Soc. Mar. Environ. Energy.* **2002**, *24*, 477–488.
27. Oh, H.J.; Lee, Y.H.; Yang, J.H.; Kim, S.H. The Characteristics of Phytoplankton Distributions Related to the Oceanographic Conditions in the Southern Waters of the Korean in Summer, 2004. *J. Korean Assoc. Geogr. Inf. Stud.* **2007**, *10*, 40–48.
28. Noh, I.H.; Yoon, Y.H.; Park, J.S.; Kang, I.S.; An, Y.K.; Kim, S.H. Seasonal fluctuations of marine environment and phytoplankton community in the southern part of Yeosu, Southern Sea of Korea. *J. Korean Soc. Mar. Environ. Eng.* **2010**, *13*, 151–164.
29. Baek, S.H.; Shin, K.S.; Hyun, B.G.; Jang, P.G.; Kim, H.S.; Hwang, O.M. Distribution Characteristics and Community Structure of Phytoplankton in the Different Water Masses During Early Summer of Southern Sea of Korea. *Ocean Polar Res.* **2010**, *32*, 1–13. [CrossRef]
30. Jang, P.G.; Hyun, B.G.; Cha, H.G.; Chung, H.S.; Jang, M.C.; Shin, K.S. Seasonal Variation of Phytoplankton Assemblages Related to Surface Water Mass in the Eastern Part of the South Sea in Korea. *Ocean Polar Res.* **2013**, *35*, 157–170. [CrossRef]
31. Rines, J.E.B.; Hargraves, P.E. The Chaetoceros Ehrenberg (Bacillariophyceae) Flora of Narragansett Bay. *Rhode Island. Bibl. Phycol.* **1988**, *79*, 196.
32. Round, F.E.; Crawford, R.M.; Mann, D.G. The diatoms. In *Biology and Morphology of the Genera*; Cambridge University Press: Cambridge, UK, 1990; p. 747.
33. Shim, J.H. Illustrated encyclopedia of flora & fauna of Korea. In *Marine Phytoplankton*; Ministry of Education Republic of Korea: Seoul, Republic of Kore, 1994; Volume 34. (In Korean)
34. Tomas, C.R. *Identifying Marine Diatoms and Dinoflagellates*; Academic Press, Inc.: Cambridge, MA, USA, 1997; p. 874.
35. Parsons, T.R.; Maita, Y.; Lalli, C.M.A. *Manual of Biological and Chemical Methods for Seawater Analysis*; Pergamon Press: Oxford, UK, 1984.
36. Bricaud, A.; Claustre, H.; Ras, J.; Oubelkheir, K. Natural variability of phytoplanktonic absorption in oceanic waters: Influence of the size structure of algal populations. *J. Geophys. Res.* **2004**, *109*, C11010. [CrossRef]
37. Fu, M.Z.; Wang, Z.L.; Li, Y.; Li, R.X.; Sun, P.; Wei, X.H.; Lin, X.Z.; Guo, J.S. Phytoplankton biomass size structure and its regulation in the Southern Yellow Sea (China): Seasonal variability. *Cont. Shelf Res.* **2009**, *29*, 2178–2194. [CrossRef]
38. Baek, S.H.; Kim, Y.B. Influences of coastal upwelling and time lag on primary production in offshore waters of Ulleungdo-Dokdo during spring 2016. *Korean J. Environ. Biol.* **2018**, *36*, 156–164. [CrossRef]
39. Liu, X.; Wang, M.; Shi, W. A study of a Hurricane Katrinainduced phytoplankton bloom using satellite observations and model simulations. *J. Geophys. Res.* **2009**, *114*, C03023.
40. Matsuda, O.; Nishi, Y.; Yoon, Y.H.; Endo, T. Observation of thermohaline structure and phytoplankton biomass the shelf front of East China Sea during early summer. *J. Fac. Appl. Biol. Sci.* **1989**, *28*, 27–35.
41. Dortch, Q.; Whitledge, T.E. Does nitrogen or silicon limit phytoplankton production in the Mississippi River plume and nearby regions? *Cont. Shelf Res.* **1992**, *12*, 1293–1309. [CrossRef]
42. Justic, D.; Rabalais, N.N.; Turner, R.E.; Dortch, Q. Changes in nutrient structure of river-dominated coastal water: Stoichiometric nutrient balance and its consequences. *Estuar. Coast. Shelf Sci.* **1995**, *40*, 339–356. [CrossRef]
43. Wang, B.D.; Wang, X.L.; Zhan, R. Nutrient conditions in the Yellow Sea and the East China Sea. *Estuar. Coast. Shelf Sci.* **2003**, *58*, 127–136. [CrossRef]
44. Yoon, Y.H.; Park, J.S.; Soh, H.Y.; Hwang, D.O. On the Marine Environment and Distribution of Phytoplankton Community in the Northern East China Sea in Early Summer 2004. *J. Korean Soc. Mar. Environ. Energy* **2005**, *8*, 100–110.
45. Zhou, M.J.; Shen, Z.L.; Yu, R.C. Responses of a coastal phytoplankton community to increased nutrient input from the Changjiang (Yangtze) River. *Cont. Shelf Res.* **2008**, *28*, 1483–1489. [CrossRef]
46. Chen, Y.L.; Lu, H.; Shiah, F.; Gong, G.; Liu, K.; Kanda, J. New production and f-ratio on the continental shelf of the East China Sea: Comparisons between nitrate inputs from the subsurface Kuroshio Current and the Changjiang River. *Estuar. Coast. Shelf Sci.* **1999**, *48*, 59–75. [CrossRef]
47. Choi, H.C.; Kang, Y.S.; Jeon, I.S. Phytoplankton Community in Adjacent Waters of Ulchin Nuclear Power Plant. *Korean J. Environ. Biol.* **2004**, *22*, 426–437.
48. Kang, Y.S.; Choi, H.C.; Lim, J.W.; Jeon, I.S.; Seo, J.H. Dynamics of the Phytoplankton Community in the Coastal Waters of Chuksan Harbor, East Sea. *Algae* **2005**, *20*, 345–352. [CrossRef]

49. Kwon, O.Y.; Kang, J.H. Seasonal Variation of Physico-chemical Factors and Size-fractionated Phytoplankton Biomass at Ulsan Seaport of East Sea in Korea. *J. Korean Acad. Ind. Coop. Soc.* **2013**, *14*, 6008–6014.
50. Magazzu, G.; Decembrini, F. Primary production, biomass and abundance of phototrophic picoplankton in the Mediterranean Sea: A review. *Aquat. Microb. Ecol.* **1995**, *9*, 97–104. [CrossRef]
51. Agawin, N.S.R.; Duarte, C.M.; Agusti, S. Nutrient and temperature control of the contribution of picoplankton to phytoplankton biomass and production. *Limnol. Oceanogr.* **2000**, *45*, 591–600. [CrossRef]
52. Zohary, T.; Brenner, S.; Krom, M.D.; Angel, D.L.; Kress, N.; Li, W.K.W.; Neori, A.; Yacobi, Y.Z. Buildup of microbial biomass during deep winter mixing in a Mediterranean warm-core eddy. *Mar. Ecol. Prog. Ser.* **1998**, *167*, 47–57. [CrossRef]
53. Decembrini, F.; Caroppo, C.; Azzaro, M. Size structure and production of phytoplankton community and carbon pathways channeling in the southern Tyrrhenian Sea (western Mediterranean). *Deep Sea Res. 2 Top. Stud. Oceanogr.* **2009**, *56*, 687–699. [CrossRef]
54. Kwak, J.H.; Lee, S.H.; Hwan, J.; Suh, Y.S.; Park, H.J.; Chang, K.I.; Kim, K.R.; Kang, C.K. Summer primary productivity and phytoplankton community composition driven by different hydrographic structures in the East/Japan Sea and the Western Subarctic Pacific. *J. Geophys. Res. Oceans* **2014**, *119*, 4505–4519. [CrossRef]
55. Son, Y.B.; Ryu, J.H.; Noh, J.H.; Ju, S.J.; Kim, S.H. Climatological variability of satellite-derived sea surface temperature and chlorophyll in the south sea of Korea and East China Sea. *Ocean Polar Res.* **2012**, *34*, 201–218. [CrossRef]
56. Shim, J.H.; Yeo, H.G.; Shin, Y.K. Ecological effect of thermal effluent in the Korean coastal waters I. Significance of autotrophic nano and picoplankton in adjacent waters of Kori nuclear power plant. *J. Oceanol. Soc. Korea* **1991**, *26*, 77–82.
57. Shim, J.H.; Yeo, H.G.; Park, J.G. Primary production system in the southern waters of the east Sea, Korea I. Biomass and productivity. *J. Oceanol. Soc. Korea* **1991**, *27*, 91–100.
58. Revelante, N.; Gilmartin, M. The relative increase of larger phytoplankton in a subsurface chlorophyll maximum of the northern Adriatic Sea. *J. Plankton Res.* **1995**, *17*, 1535–1562. [CrossRef]
59. Marañón, E.; Holligan, P.M.; Barciela, R.; González, N.; Mouriño, B.; Pazó, M.J.; Varela, M. Patterns of phytoplankton size structure and productivity in contrasting open-ocean environments. *Mar. Ecol. Prog. Ser.* **2001**, *216*, 43–56. [CrossRef]
60. Morán, X.A.G.; Taupier-Letage, I.; Vázquez-Domínguez, E.; Ruiz, S.; Arin, L.; Raimbault, P.; Estrada, M. Physical-biological coupling in the Algerian Basin (SW Mediterranean): Influence of mesoscale instabilities on the biomass and production of phytoplankton and bacterioplankton. *Deep Sea Res. 1 Oceanogr. Res. Pap.* **2001**, *48*, 405–437. [CrossRef]
61. Ning, X.; Chai, F.; Xue, H.; Cai, Y.; Liu, C.; Shi, J. Physical-biological oceanographic coupling influencing phytoplankton and primary production in the South China Sea. *J. Geophys. Res.* **2005**, *110*, C10005. [CrossRef]
62. Raven, J.R. The twelfth tansley lecture. Small is beautiful: The picophytoplankton. *Funct. Ecol.* **1998**, *12*, 503–513. [CrossRef]
63. Litchman, E.; Klausmeier, C.A.; Schofield, O.M.; Falkowski, P.G. The role of functional traits and trade-offs in structuring phytoplankton communities: Scaling from cellular to ecosystem level. *Ecol. Lett.* **2007**, *10*, 1170–1181. [CrossRef] [PubMed]
64. Longhurst, A.R. *Ecological Geography of the Sea*; Academic Press: London, UK, 2010.
65. Lee, S.H.; Joo, H.T.; Lee, J.H.; Lee, J.H.; Kang, J.J.; Lee, H.W.; Lee, D.B.; Kang, C.K. Carbon uptake rates of phytoplankton in the Northern East/Japan Sea. *Deep Sea Res. 2 Top. Stud. Oceanogr.* **2017**, *143*, 45–53. [CrossRef]
66. Gong, G.C.; Wen, Y.H.; Wang, B.W.; Liu, G.J. Seasonal variation of chlorophyll a concentration, primary production and environmental conditions in the subtropical East China Sea. *Deep. Res. 2 Top. Stud. Oceanogr.* **2003**, *50*, 1219–1236. [CrossRef]
67. Zhang, Y.R.; Ding, Y.P.; Li, T.J.; Xue, B.; Euo, Y.M. Annual variations of chlorophyll a and primary productivity in the East China Sea. *Oceanol. Limno. Sin.* **2016**, *47*, 261–268.
68. Nagata, H. The Yamato Rise, central Japan Sea. *Plankton Bio. Ecol.* **1998**, *45*, 159–170.
69. Yoshie, N.; Shin, K.H.; Noriki, S. Seasonal variations of primary productivity and assimilation numbers in the western North Pacific. *Spec. Rep. Reg. Stud. North-East Eurasia North Pac. Hokkaido Univ.* **1999**, *1*, 49–62.
70. Kang, Y.S.; Choi, J.K.; Chung, K.H.; Park, Y.C. Primary productivity and assimilation umber in the Kyonggi bay and the mid-eastern coast of Yellow Sea. *J. Oceanogr. Soc. Korea.* **1992**, *27*, 237–246.
71. Jang, H.K.; Kang, J.J.; Lee, J.H.; Kim, M.; Ahn, S.H.; Jeong, J.Y.; Yun, M.S.; Han, I.S.; Lee, S.H. Recent Primary Production and Small Phytoplankton Contribution in the Yellow Sea during the Summer in 2016. *Ocean Sci. J.* **2018**, *53*, 509–519. [CrossRef]
72. Richardson, A.J. In hot water: Zooplankton and climate change. *ICES J. Mar. Sci.* **2008**, *65*, 279–295. [CrossRef]
73. Hansen, B.; Hjornsen, P.K.; Hansen, P.J. The Size Ration between Planktonic Predators and Their Prey. *Limmol. Oceanogr.* **1994**, *39*, 395–403. [CrossRef]
74. Calbet, A.; Landary, M.R. Mesozooplankton Influences on the Microbial Food Web: Direct and Indirect Trophic Interactions in the Oligotrophic Open Ocean. *Limmol. Oceanogr.* **1999**, *44*, 1370–1380. [CrossRef]
75. Yang, E.J.; Choi, J.K. Ingestion on Planktonic Ciliates by Copepod Acartia Hongi: A Laboratory Study. *Ocean Polar Res.* **2009**, *31*, 265–276. [CrossRef]